communications earth & environment

Article

https://doi.org/10.1038/s43247-024-01443-2

Submarine volcanic microbiota record three volcano-induced tsunamis

Hoil Lee [1], Yire Choi [1] ✉, Ji Hye Han [2], Sang Deuk Lee [2], Sujeong Park[1] & Jin-Hyuck Choi[1]

The precise determination of sediment provenance not only yields insights into past tsunami events but also offers a window into understanding the genesis of tsunamis in distinct environments, such as volcanic regions. Through meticulous analysis of core samples from a lagoon in east of Korea Peninsula, we unveil three previously undocumented tsunamis and identify specific bacterial taxa associated with submarine volcanism during distinct periods. Specific bacterial species (*Sulfurimonas*_f and *Alicyclobacillus ferrooxydans*) and the presence of the silicoflagellate *Dictyocha byronalis* indicate deep-sea volcanic origins for certain sediment layers. The presence of microfossils, typically found in high-salinity pelagic environments during Event I, strongly supports the occurrence of a tsunami. These findings align with heightened volcanic activity on Ulleung Island during Event I and provide valuable chronological insights into submarine volcanic processes near Ulleung Island for Events II and III. Our study highlights these biological markers as crucial indicator for understanding past tsunamis arising from volcanic activity.

A destructive tsunami warning was issued at the Pacific coastal areas as a consequence of the eruption of the Hunga Tonga–Hunga Ha'apai submarine volcano (20.54°S, 175.38°W) on 15 January 2022. This occurrence suggests that tsunamis resulting from submarine volcanic activity can impact remote regions as well[1]. This event constitutes a devastating natural disaster with the potential to inflict extensive destruction and casualties.

Tsunamis are commonly triggered by extensive seismic events, primarily large-scale earthquakes[2,3]. Such subaqueous disruptions generate seismic waves that radiate outward from the epicenter and eventually reach shallower coastal waters, culminating in the formation of a tsunami[4]. In addition to seismic activity, tsunamis can also be induced by submarine volcanic eruptions or landslides[5,6]. These alternate sources can amplify the vulnerability of coastal regions to tsunamis, as their emergence lacks the characteristic seismic ground motions typically associated with major earthquakes, making them challenging to predict[7–11].

Extensive insights into the occurrence, chronological context, and physical attributes of tsunami sediments have been gleaned through research on tsunami deposits, particularly following the catastrophic tsunamis triggered by the 2004 Sumatra earthquake and the 2011 Tohoku–Oki earthquake[12–19]. Furthermore, considerable proxy indicators derived from analyses of contemporary tsunami deposits have been introduced as tools for the recognition of tsunami-related sediments within coastal sediment archives[20–24].

Nevertheless, cases of ambiguity in interpretation exist due to the origin of the sediments and their similarities with other sedimentary processes[25–27]. Consequently, to mitigate this interpretational uncertainty, a precise elucidation of the sedimentary composition originating from the tsunami's source becomes indispensable.

In this context, tsunamis triggered by submarine volcanic eruptions may exhibit distinct characteristics. For instance, the discovery of highly specialized bacteria indigenous to underwater volcanoes or associated hydrothermal vents in a significantly disparate environment, far removed from coastal areas, could present compelling evidence of a tsunami occurrence. Such findings can serve as clear indicators for interpreting the presence of a tsunami, potentially offering a vital means to elucidate and trace its occurrence.

Over the past 2000 years of recorded tsunami history around the East Sea, a significant proportion of these events tend to have occurred primarily in the eastern part of Japan, precisely along the plate boundary. Meanwhile, records of tsunamis within the East Sea itself are notably infrequent (Fig. 1, National Centers for Environmental Information, https://www.ngdc.noaa.gov). Furthermore, most of the origins of tsunamis in the East Sea are reported as earthquakes. Despite exhibiting robust indicators of active volcanic activity, including the conspicuous presence of multiple submarine volcanoes and volcanic islands, the extant body of knowledge pertaining to the volcanic origins within the designated area remains considerably limited[28–30]. The East Sea presents a distinctive geostrategic advantage due to its semi-closed configuration. This geographical trait not only serves to mitigate the intricacies entailed in the process of retracing its geological genesis but also engenders a conducive setting for scholarly pursuits. The

[1]Korea Institute of Geoscience and Mineral Resources (KIGAM), 124 Gwanhak-ro, Yuseong-gu, Daejeon 34132, Republic of Korea. [2]Nakdonggang National Institute of Biological Resources (NNIBR), Donam 2-gil 137 (Donam-dong), Sangju-si, Gyeongsangbuk-do, Republic of Korea. ✉e-mail: ir_1254@kigam.re.kr

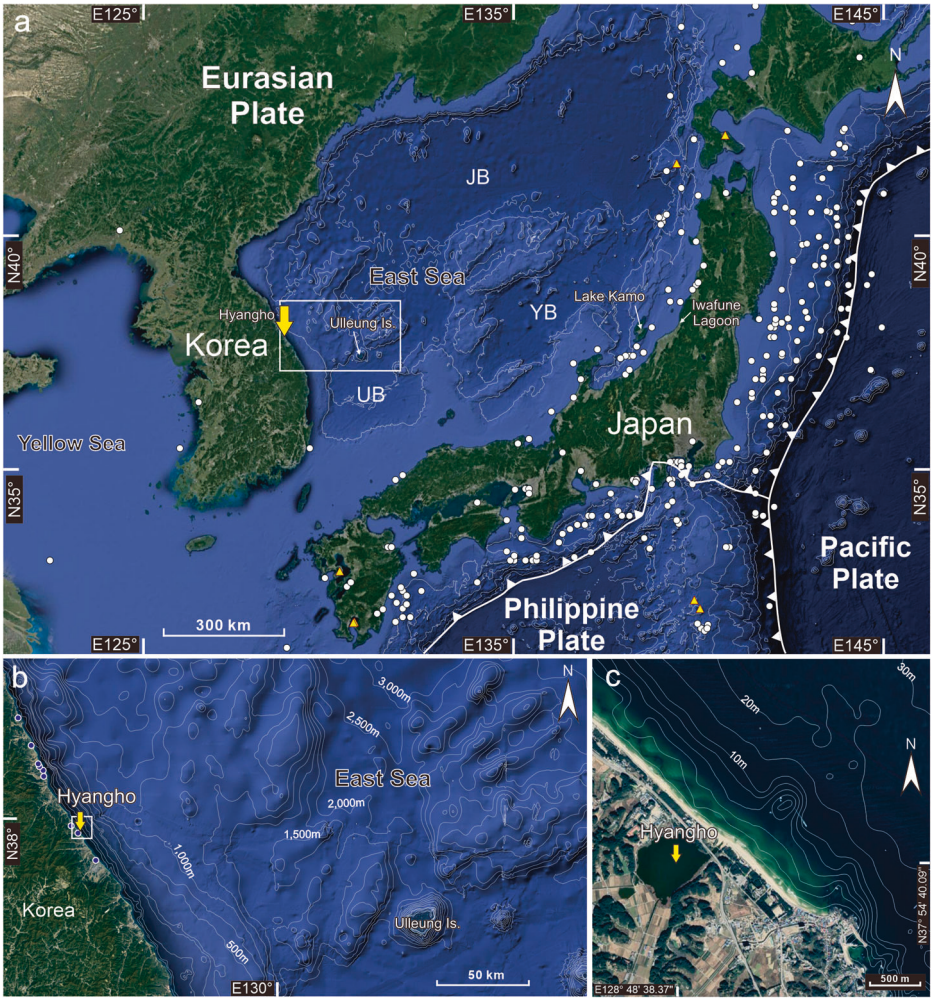

Fig. 1 | Map of the study site and its surrounding historical tsunami sources. a The study area corresponds to the central part of the eastern coast of the Korean Peninsula, and the Pacific Plate and the Philippine Plate boundaries are located to the east and southeast of the study area. In reference to these plate boundary subduction zones, the East Sea is referred to as a back-arc basin and consists of the Ulleung Basin (UB), Japan Basin (JB), and Yamato Basin (YB). The sources of the tsunamis over the last 2000 years (white circles: earthquakes; yellow triangles: volcanoes) are common not only in the eastern part of Japan but also in the western part of Japan (National Centers for Environmental Information, https://www.ngdc.noaa.gov). **b** The study area, Lagoon Hyangho, is an area that faces the Ulleung Basin, and the water depth rapidly increases offshore. Ulleung Island, which is located in the Ulleung Basin, is an island formed by volcanic activity, and the undersea topography has developed via volcanic activity in the East Sea[30]. The blue circles indicate the locations of the lagoons. **c** Lagoon Hyangho has an average depth of approximately 2 m. Unlike the tide level on the western coast, which is extremely high, the tidal level on the eastern coast is less than 0.5 m. The yellow arrow indicates the drilling location of core 20HH01. (Map data ©2020 Google).

containment offered by the semi-closed expanse augments the prospect of meticulous volcanic investigations while concurrently fostering the potential for the safeguarding of pivotal geological archives, owing to the diminished scope of extraneous perturbations.

The aim of this study is to unveil geological evidence of a tsunami triggered by a volcanic eruption in the East Sea, with the intent of enhancing the discernment of tsunami sediments. Additionally, this research seeks to introduce a novel criterion for tracing sediments originating from volcanic-induced tsunamis. It can provide further insights to researchers in the field of tsunami-related studies and contribute to the advancement of research techniques in this regard.

Results and discussion

Sedimentary and biological evidence for tsunami deposits

While maximum tsunami wave heights of 3 to 4 m were observed in 1983 and 1993 along the middle of the eastern coast of Korea[31], the deposits from these tsunamis are not discernible in the lagoon sediments of Hyangho (20HH01), located in the middle of the eastern coast (Figs. 1 and 2). There are several possible reasons for this, and one plausible reason is that the energy generated by these tsunamis might not have been sufficiently potent to precipitate typical tsunami sand accumulation in our study site (Fig. 1). Consequently, substantial quantities of tsunami sand might not have traversed the coastal sand bar of the lagoon. In the event that some sand did breach the sandbar, it is probable that it settled on the seaward side of the lagoon[4].

However, the biological signals in our sample, collected from Hyangho, yielded intriguing results through analyses bacterial diversity and microfossil analyses. The bacterial diversity analysis revealed that the genus *Thiomicrohabdus* and *Thiomicrospira* (Gammaproteobacteria) were major constituents (avg. 38.31%) in samples taken from most of the sediment depths, although certain depths exhibited high proportions of Epsilonproteobacteria (Supplementary Data 2–6). Especially, the *Sulfurimonas*_f, an uncultured *Sulfurimonas* species under the class Epsilonproteobacteria, manifested at specific strata: avg. 6.21% in 11.77–11.10 m (ca. 8.8–8.3 ka; Event I), avg. 20.43% in 9.23–8.10 m (ca. 7.8–6.5 ka; Event II), and avg. 8.69% in 2.30–1.20 m (ca. 2.5–0.3 ka; Event III) (Fig. 3). *Sulfurimonas*_f were often found in hydrothermal vents[32–38], although they were ubiquitous in diverse marine and terrestrial environments and especially abundant in sulfur-enrich environment[35–37]. Bacterial mats belonging to the *Sulfurimonas*_f are commonly encountered on seamounts resulting from intense volcanic activity linked to underwater volcanoes and hydrothermal vents[38,39]. In order to compare with sequences from various environments, representative 16 S rRNA gene sequences were extracted from depths where *Sulfurimonas*_f was present in a high proportion. As a result of the blast and phylogenetic analysis using a representative sequence, it was confirmed that the closest sequence was the clone sequence collected from the marine hydrothermal vent fluid. The results of this phylogenetic analysis support that the origin of the representative sequence analyzed from the lagoon sediments can be inferred to be a marine hydrothermal vent.

Similarly, *Alicyclobacillus ferrooxydans* (Firmicutes) showed a high proportion of 6.8% in the normalized data and 9.8% in the original data only at a depth of 11.23 m (ca. 8.3 ka) (Fig. 3). This particular taxon is primarily encountered within acidic, geothermal environments and can withstand

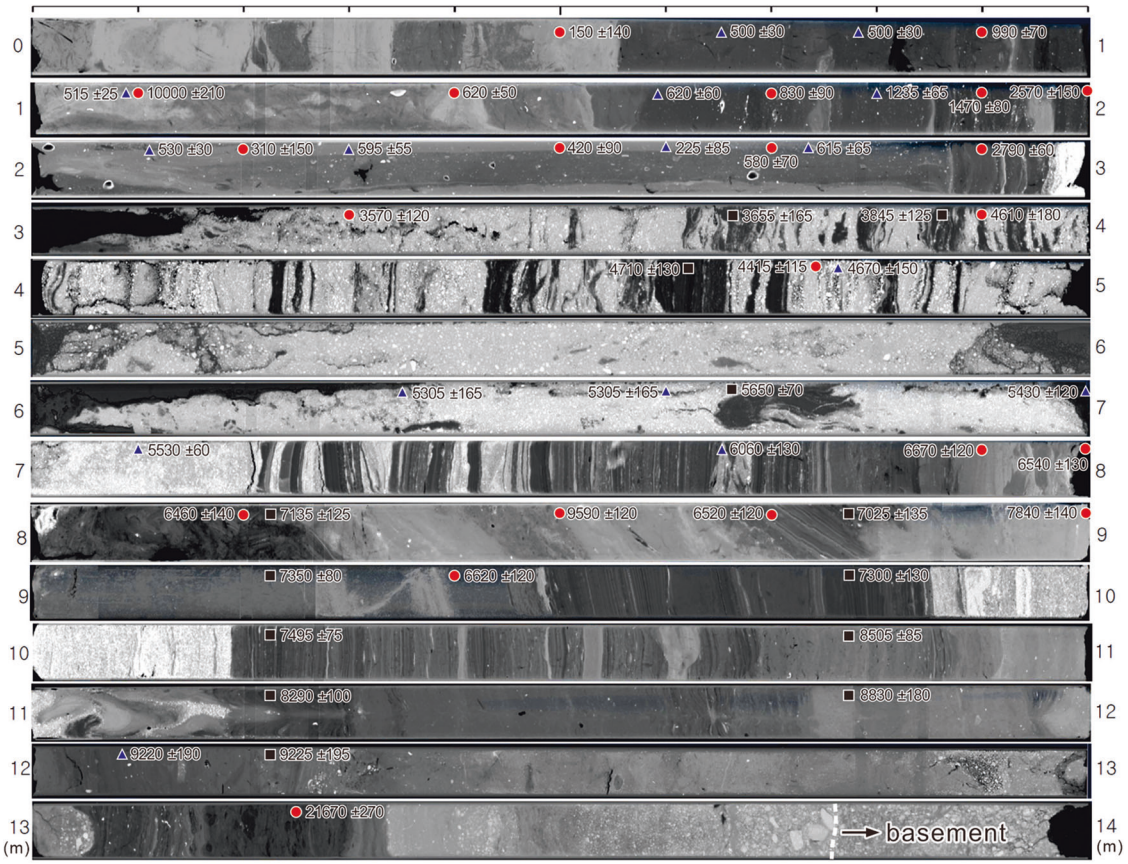

Fig. 2 | Computed tomography (CT) image of core 20HH01. The calibrated AMS ^{14}C ages are shown in the core images (red circles mark plants, blue triangles indicate shells, and black squares show bulk sediment).

extreme environments by forming endospores[40]. *Alicyclobacillus ferrooxydans* was first isolated from the soil of a volcanic region that spews sulfur gas and steam in Tengchong City, China, which is famous for volcanic activity[40].

Microfossil analysis reveals that the majority of microfossils indicate a coastal environment. However, the presence of the silicoflagellate *Dictyocha byronalis* at a depth of 11.23 m presents an anomaly (Fig. 3, Supplementary Data 7). Despite limited studies on *Dictyocha byronalis*, a newly observed taxon in Korea through this investigation has shown that it is typically dominant in environments characterized by relatively warm temperatures and high salinity[41,42].

The above biological results reveal that most taxa in core 20HH01 live in nearshore environments, including freshwater environments (Supplementary Data 2–7). Nevertheless, *Sulfurimonas*_f, *Alicyclobacillus ferrooxydans* and *Dictyocha byronalis*, which are present only at specific depths, do not indicate a nearshore environment. Consequently, their presence is interpreted as supplied from the distant sea.

Interestingly, a thin layer of sand was noted at a depth of 11.20 m (ca. 8.3 ka) (Fig. 3). This layer holds the potential to be indicative of sand delivered by a tsunami, as substantiated by biological evidence. Additionally, at depths ranging from 8.8 to 8.1 m (ca. 7.1–6.5 ka), prominently deformed laminations are frequently observed (Fig. 3). These deformations might have arisen due to gravitational instability, potentially triggered by events such as earthquakes or tsunamis.

The three intervals (Event I, Event II, and Event III) proposed in this article as potential tsunami occurrences collectively exhibit physical and biological characteristics that indicate transient events, as opposed to reflecting general environmental changes.

To explore another option that may explain the data, the most common coastal events that are frequently compared to tsunamis are coastal storms resulting from typhoons[43,44]. Indeed, the edge of the Pacific high-pressure system is frequently located over the Korean Peninsula, including Hyangho, in summer and autumn, and as such, Hyangho is frequently in the path of typhoons[45,46]. Nevertheless, explaining typhoons as one of the plausible mechanisms that caused the specific intervals identified in this study poses a challenge, considering that typhoons occur multiple times a year in this region. Additionally, the impact of a robust typhoon's high storm wave base on the lower shoreface is recognized[47,48]; typhoons are unlikely to affect depths of thousands of meters in the East Sea.

Interestingly, within the intervals of Event II and Event III, the ages are both approximately 10.0–9.6 ka, which is approximately 2000 years older than the surrounding sediment for Event II and 8000 years older than the surrounding sediment for Event III (Fig. 3). In particular, in the Event III age group, charcoal older than 8000 years is very difficult to deposit via sedimentary processes on land because the ages are usually between hundreds of years and 1000 years. The prevailing assumption is that this material potentially originated from a pelagic ocean tsunami characterized by a remarkably low sedimentation rate.

What was the source of the tsunamis?

*Sulfurimonas*_f, which is detected in three sections in core 20HH01, is regarded as a major component of microbial communities at deep-sea vents and plays an important role in the biogeochemical cycle of hydrothermal vent[38]. Several studies reported that the microbiome of hydrothermal vents[32,34,35,49,50] commonly described Epsilonproteobacteria (especially *Sulfurimonas*) as a major component of hydrothermal vents. In particular, German et al.[35] showed *Sulfurimonas* have been detected at hydrothermal vents, in plume samples, and in marine sediments but not in surface seawater. Additionally, Spietz et al.[33] showed very interesting results between *Sulfurimonas* and volcano lava. They reported a significant increase in the relative abundance of Epsilonproteobacteria (including *Sulfurimonas sp.*) in hydrothermal plumes over the lava flow, and this bacterial taxon could be a strong indicator of hydrothermal activity. Eruptions can generate new

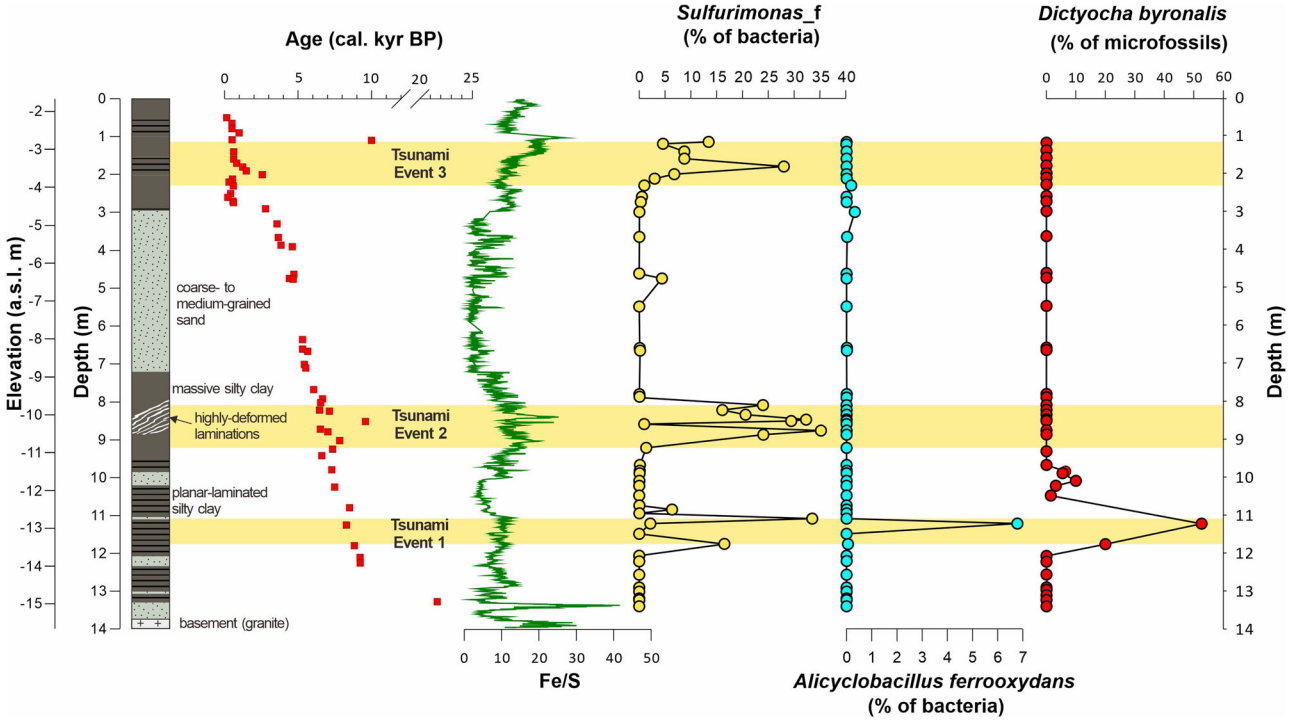

Fig. 3 | Inferred three tsunami events in core 20HH01. The stratigraphy of the study area (left) is dominated by silty clay interspersed with sand. In particular, highly deformed laminations appear at depths of approximately 8–9 m (refer to Fig. 2). The age results show that the sediments are thousands of years older than the surrounding sediments at depths of 1.1 m and 8.5 m supplied by tsunami events from the pelagic ocean. The excursions in the Fe/S profile correlate with the appearance of *Sulfurimonas*_f and are consistent with the anomalous AMS ^{14}C ages in this core. The appearance of abundant *Alicyclobacillus ferrooxydans* and *Dictyocha byronalis* in Event I indicates that *Sulfurimonas*_f was related to volcanic activity.

releases of hydrothermal fluids due to new heat sources such as seafloor magma and newly erupted lava fields, and the indicator microbes in these thermal vents may be inferred to be associated with volcanic activity (such as an eruption). However, this inference also has limitations that must be sufficiently proven through culture and genome analysis.

The source areas of the tsunamis in the study area can essentially be constrained to the East Sea or its vicinity, such as Ulleung Island. The East Sea, which is adjacent to a plate boundary, has experienced frequent earthquakes and volcanic eruptions (Fig. 1). While Ulleung Island, which is located in the Ulleung Basin, contains volcanic records that are representative of the East Sea, there are also large and small volcanoes distributed on the seabed in the Ulleung Basin[30,51,52].

As the East Sea contains several submarine volcanoes, it is difficult to specify a particular volcanic source area. Nevertheless, Event I (ca. 8.3 ka), when volcanic activity is inferred to have occurred, coincides chronologically with a known eruption period (U-3 or N-3; tephra layer) on Ulleung Island (Fig. 4)[28,29,53]. Therefore, the ca. 8.3 ka tsunami is likely related to an eruption of Ulleung Island, at a minimum, rather than other volcanic activity in the East Sea (Fig. 4). This eruption took place on the existing Ulleung Island[53], but the appearance of the *Sulfurimonas*_f and *Alicyclobacillus ferrooxydans* indicates that volcanic activity occurred in the surrounding seabed during this episode of Ulleung Island's volcanic eruption.

Moreover, because ash fallout can significantly increase the Fe content in the surface ocean, the Fe content in sediments can be used as an indicator of volcanic activity[54–59]. Thus, the volcanic eruptions on Ulleung Island during the Holocene were recorded as changes in the Fe content in sediments. The Fe/S values of the core were determined using an XRF core scanner to confirm the trend of Fe fluctuations. The value is determined after removing the influence of pyrite because Fe and S are elements constituting pyrite produced by sulfate-reducing bacteria in an anoxic environment[60–63]. As shown by the results, the patterns of Fe/S and *Sulfurimonas*_f variation tend to increase together during the three events (Fig. 3). This correlation implies the potential transportation of Fe-rich sediments and hydrothermal bacteria to the eastern coast of Korea through tsunamis engendered by volcanic eruptions around the Ulleung Basin.

Influence of tsunami events generated by volcanism and application as a key indicator

A tsunami generated in the East Sea is very likely to impact not only the coast of Korea but also the western coast of Japan. Unfortunately, research on tsunamis in Japan has mostly focused on the eastern coast of Japan bordering the Pacific Ocean[64], and only a few studies have focused on the western coast of Japan facing the East Sea[65]. Urabe[65] reported twenty-four events in Lake Kamo and nine events in Iwafune Lagoon that were determined to be related to tsunamis on the western coast of Japan during the past 9000 years. We correlated their age dating results of the sedimentary layers associated with each event with our results: Event I corresponds to Ev24 to Ev22 in Lake Kamo and Ev9 in Iwafune Lagoon, Event II corresponds to Ev20 to Ev16 in Lake Kamo and Ev7 to Ev5 in Iwafune Lagoon, and Event III corresponds to Ev6 to Ev2 in Lake Kamo and Ev1 in Iwafune Lagoon (Fig. 1a; Fig. 4).

The biological signals of this study, the *Sulfurimonas*_f, and *Alicyclobacillus ferrooxydans*, have been found only in volcanic or hydrothermal areas[36–38,40,66,67]. Their appearance in coastal lagoons unrelated to volcanic or deep-sea hydrothermal activity provide clear evidence of tsunami-driven sediments with a deep-sea volcanic origin. Consequently, these biological signals can serve as indicators of past tsunamis originating from volcanic activity. Additionally, the existence of species other than those mentioned above in deep hydrothermal environments can also serve as reliable indicators in semi-closed seas or closed lakes.

Since this study was conducted in one area of the East Sea, it is necessary to correlate the findings by securing data from other areas bordering the East Sea. Additional research on the spread of *Sulfurimonas*_f due

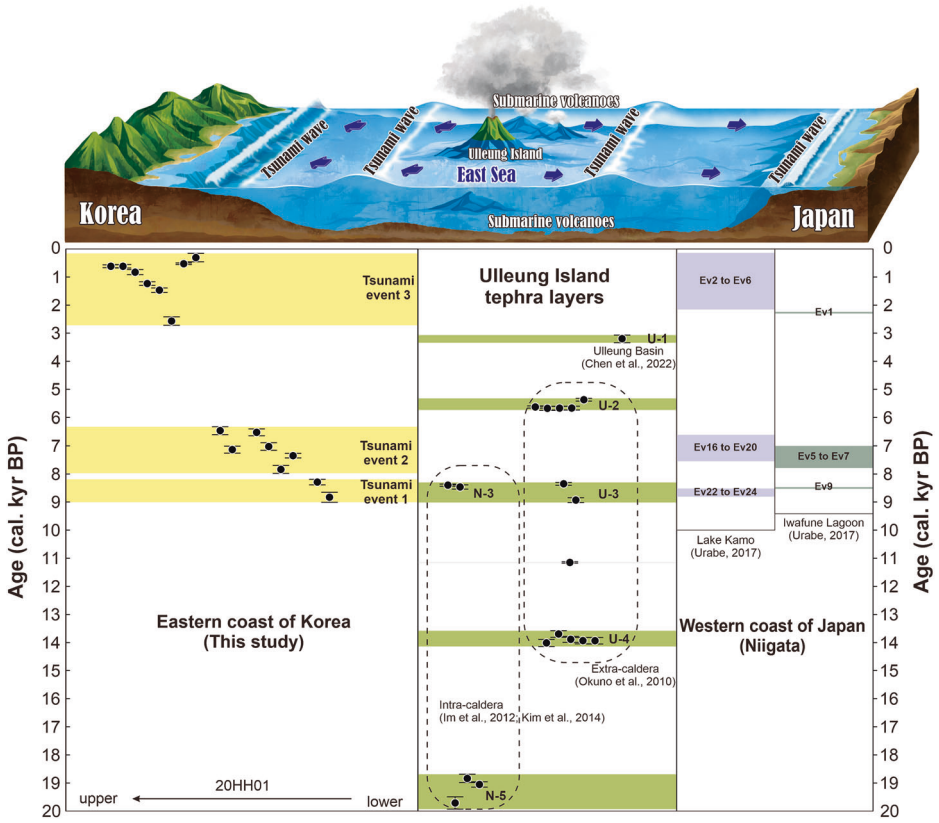

Fig. 4 | Comparison of AMS ^{14}C dating results between the tephra layers originating from Ulleung Island, the western coast of Japan, and the three intervals indicating tsunami events in the study area. Event I is correlated with tephra layer U-3 (or N-3), suggesting that this event is related to the volcanic activity on Ulleung Island. The other two tsunami events are likely related to other submarine volcanic events in the East Sea and correlate with sections on the western coast of Japan analyzed by a previous study. (The error for cal. kyr BP is ±2σ).

to volcanic eruptions is essential in wider oceanic regions beyond the geographically semi-enclosed East Sea.

Methods

The drilling (date: 08 December 2020) was performed from a barge in lagoon Hyangho (128°48′38.37″E, 37°54′40.09″N, 1.7 m in water depth), and a core with a total length of 14 m was extracted from the sediment-water interface of Hyangho lagoon to the bedrock. The sediments core recovered using a PVC pipe were cut into half vertically, and sub-sampling was performed for age dating, bacterial and microfossil analyses (Fig. 2).

Age dating was carried out by accelerator mass spectrometry (AMS) at the Korean Institute of Geoscience and Mineral Resources (KIGAM), Korea, using plants, shells, and humic materials. The calibration ages were corrected by the OxCal statistical analysis program (http://c14.arch.ox.ac.uk, Supplementary Data 1).

Soil genomic DNA was extracted from 0.25 g of sediment using a DNeasy PowerSoil Pro Kit (Qiagen) according to the manufacturer's instructions. The sampling depths are shown in Supplementary data 2. The polymerase chain reaction (PCR) primer pair 16S-F (5′-CCTACGGGNGGCWGCAG-3′)/16S-R (5′-GACTACHBGGGTATCTAATCC-3′) was used to amplify the V3–V4 hypervariable regions of the 16 S rRNA gene[68]. KAPA HiFi HotStart ReadyMix (KAPA Biosystems) and Agencourt AMPure XP system (Beckman Coulter Genomics) were used for PCR amplification and purification of the PCR product, respectively. PCR conditions were performed as follows: initial denaturation at 95 °C for one min, 34 cycles of 95 °C for 30 s, 55 °C for 30 s, 72 °C for 30 s, followed by a final extension at 72 °C for 5 min. Purification of the PCR product was carried out according to the manufacture's protocol.

After magnetic bead-based purification of PCR products, the second PCR was conducted using primers from a Nextera XT Index Kit (Illumina). Subsequently, purified PCR products were visualized using gel electrophoresis and quantified with a Qubit dsDNA HS Assay Kit (Thermo Scientific) on a Qubit 3.0 fluorometer. The pooled samples were qualified by running on an Agilent 2100 bioanalyzer (Agilent) and quantified by qPCR using a CFX96 Real-Time System (Bio-Rad). After normalization, Illumina MiSeq sequencing was performed at Bionics, Korea. The 16 S rRNA gene sequence was identified in EZbioCloud using the Microbiome Taxonomic Profiling (MTP) pipeline (https://www.ezbiocloud.net, CJ Bioscience)[69,70]. Quality control of raw data was performed according to CJ Bioscience's in-house process). The bacterial OTUs were identified by UCLUST[71], clustering of the 16 S rRNA sequences with a ≥ 97% identity threshold, for taxonomic profiling analysis. The PKSSU4.0 database included in EzBioCloud was used for the taxonomic assignment of all reads. Bacterial compositions were assessed, and α-diversity indices were calculated (Chao1, ACE, Shannon, and Simpson). Also, the bacterial diversity of sediment samples was compared using normalization to 10,000 read counts to minimize sequencing bias.

All raw 16 S rRNA gene sequencing data were deposited in the NCBI Sequence Read Archive (SRA) under accession number SRR27371705-SRR27371753 (BioProject PRJNA1058190). There were 42 microfossil samples taken from core 20HH01. Microfossil analysis on these samples was conducted according to the following steps: 1 g of sediment was dried at 60 °C for 24 h, the siliceous material was boiled with 20 mL of 30% hydrogen peroxide (H_2O_2) and washed with distilled water to remove organic matter, and the treated samples were mounted with Pleurax (Mountmedia, Wako, Japan) and briefly heated using an alcohol lamp for subsequent analysis with a light microscope (LM; Eclipse Ni, Nikon, Tokyo, Japan). Photomicrographs were taken using a digital camera (DS-Ri2, Nikon, Tokyo, Japan). Some remaining peroxide-cleaned samples were filtered using 2.0-μm polycarbonate membrane filters (Nuclepore, Whatman, Maidstone, UK). The membranes were placed on stubs and coated with gold–palladium for analysis using field emission scanning electron microscopy (FE-SEM; MIRA 3, TESCAN, Brno-Kohoutovice, Czech Republic). SEM photomicrographs of all the samples were used to identify the microfossils. Morphological analyses of microfossils were performed using ImageJ v1.32 software

(NIS-Elements BR4.50.00, Nikon, Tokyo, Japan). Microfossils were taxonomically identified primarily by referring to the literature[72–75].

To obtain continuous and high-resolution elemental information, we used the X-ray fluorescence (XRF) core scanner at the KIGAM (Avvatech B.V., Alkmaar, Netherlands). The surfaces of the split-opened core 20HH01 were covered with SPEXCerti Ultralend foil to prevent contamination of the sensors and sediments. Two electronic conditions were used for detecting Al to Fe at 10 kV and 0.25 mA with no filter and Cu to Zr at 30 kV and 1.0 mA with a thick Pb filter. We also used ratio calibration methods, such as Sr/Ti, Si/Al, Sr/Ca, and Fe/S[76].

Reporting summary

Further information on research design is available in the Nature Portfolio Reporting Summary linked to this article.

Data availability

All data generated for this research are provided in the Supplementary Data File. The supplementary data is also uploaded on Figshare, and the link is as follows. https://doi.org/10.6084/m9.figshare.25624587.v1.

Received: 3 October 2023; Accepted: 8 May 2024;
Published online: 21 May 2024

References

1. Wright, C. J. et al. Surface-to-space atmospheric waves from Hunga Tonga–Hunga Ha'apai eruption. *Nature* **609**, 741–746 (2022).
2. Kanamori, H. Mechanism of tsunami earthquakes. *Phys. Earth Planet. Inter.* **6**, 346–359 (1972).
3. Satake, K. & Heidarzadeh, M. A review of source models of the 2015 Illapel, Chile earthquake and insights from Tsunami data. *Pure Appl. Geophys.* https://doi.org/10.1007/s00024-016-1450-5 (2017).
4. Dawson, A. G. & Stewart, I. Chapter Ten - Offshore Tractive Current Deposition: The Forgotten Tsunami Sedimentation Process. in *Tsunamiites* (eds Shiki, T., Tsuji, Y., Yamazaki, T. & Minoura, K) 153–161 (Elsevier, Amsterdam, 2008). https://doi.org/10.1016/B978-0-444-51552-0.00010-2.
5. Ward, S. N. & Day Benfield, S. *Cumbre Vieja Volcano-Potential Collapse and Tsunami at La Palma, Canary Islands 2. Geological Evidence for a Future Collapse of the Cumbre Vieja*. 28 (2001).
6. Paris, R. Source mechanisms of volcanic tsunamis. *Philos. Trans. R. Soc. A* **373**, 20140380 (2015).
7. Grilli, S. T. et al. Modelling of the tsunami from the December 22, 2018 lateral collapse of Anak Krakatau volcano in the Sunda Straits, Indonesia. *Sci. Rep.* **9**, 11946 (2019).
8. Hunt, J. E. et al. Submarine landslide megablocks show half of Anak Krakatau island failed on December 22nd, 2018. *Nat. Commun.* **12**, 2827 (2021).
9. Tappin, D. R. et al. Sediment slump likely caused 1998 Papua New Guinea tsunami. *Eos Trans. Am. Geophys. Union* **80**, 329–340 (1999).
10. Walter, T. R. et al. Complex hazard cascade culminating in the Anak Krakatau sector collapse. *Nat. Commun.* **10**, 4339 (2019).
11. Sandanbata, O. et al. Sub-decadal volcanic tsunamis due to submarine trapdoor faulting at Sumisu Caldera in the Izu–Bonin arc. *J. Geophys. Res. Solid Earth* **127**, e2022JB024213 (2022).
12. Ishimura, D. & Yamada, K. Integrated lateral correlation of tsunami deposits during the last 6000 years using multiple indicators at Koyadori, Sanriku Coast, northeast Japan. *Quat. Sci. Rev.* **256**, 106834 (2021).
13. Chatenoux, B. & Peduzzi, P. Impacts from the 2004 Indian Ocean Tsunami: analysing the potential protecting role of environmental features. *Nat. Hazards* **40**, 289–304 (2007).
14. Hawkes, A. D. et al. Sediments deposited by the 2004 Indian Ocean Tsunami along the Malaysia–Thailand Peninsula. *Mar. Geol.* **242**, 169–190 (2007).
15. Jankaew, K. et al. Medieval forewarning of the 2004 Indian Ocean tsunami in Thailand. *Nature* **455**, 1228–1231 (2008).
16. Choowong, M. et al. Flow conditions of the 2004 Indian Ocean tsunami in Thailand, inferred from capping bedforms and sedimentary structures. *Terra Nova* **20**, 141–149 (2008).
17. Mori, N., Takahashi, T., Yasuda, T. & Yanagisawa, H. Survey of 2011 Tohoku earthquake tsunami inundation and run-up. *Geophys. Res. Lett.* **38**, L00G14 (2011).
18. Saito, T., Ito, Y., Inazu, D. & Hino, R. Tsunami source of the 2011 Tohoku-Oki earthquake, Japan: Inversion analysis based on dispersive tsunami simulations. *Geophys. Res. Lett*. **38**, L00G19 (2011).
19. Norio, O., Ye, T., Kajitani, Y., Shi, P. & Tatano, H. The 2011 eastern Japan great earthquake disaster: overview and comments. *Int. J. Disaster Risk Sci.* **2**, 34–42 (2011).
20. Goff, J., McFadgen, B. G., Chagué-Goff, C. & Nichol, S. L. Palaeotsunamis and their influence on Polynesian settlement. *Holocene* **22**, 1067–1069 (2012).
21. Scheffers, A. M. Chapter 3—Paleotsunami Research—Current Debate and Controversies. in *Coastal and Marine Hazards, Risks, and Disasters* (eds Shroder, J. F., Ellis, J. T. & Sherman, D. J.) 59–92 (Elsevier, Boston, 2015). https://doi.org/10.1016/B978-0-12-396483-0.00003-0.
22. Ishizawa, T., Goto, K., Yokoyama, Y. & Miyairi, Y. Non-destructive analyses to determine appropriate stratigraphic level for dating of tsunami deposits. *Mar. Geol.* **412**, 19–26 (2019).
23. Dura, T. & Hemphill-Haley, E. *Diatoms in Tsunami Deposits*. *Geological Records of Tsunamis and Other Extreme Waves* (Elsevier Inc., 2020). https://doi.org/10.1016/b978-0-12-815686-5.00014-6.
24. Shinozaki, T. Geochemical approaches in tsunami research: current knowledge and challenges. *Geosci. Lett.* **8**, 6 (2021).
25. Montoya, L. & Lynett, P. Tsunami versus infragravity surge: comparison of the physical character of extreme runup. *Geophys. Res. Lett.* **45**, 912–982 (2018).
26. Engel, M. et al. Chapter 20 - Paleogenetic approaches in tsunami deposit studies. in *Geological Records of Tsunamis and Other Extreme Waves* (eds Engel, M., Pilarczyk, J., May, S. M., Brill, D. & Garrett, E.) 427–442 (Elsevier, 2020). https://doi.org/10.1016/B978-0-12-815686-5.00020-1.
27. Costa, P. J. et al. The application of microtextural and heavy mineral analysis to discriminate between storm and tsunami deposits. *Geol. Soc. Lond. Spec. Publ.* **456**, 167–190 (2018).
28. Okuno, M. et al. AMS Radiocarbon dating of Holocene tephra layers on Ulleung Island, South Korea. *Radiocarbon* **52**, 1465–1470 (2010).
29. Im, J. H., Shim, S. H., Choo, C. O., Jang, Y. D. & Lee, J. S. Volcanological and paleoenvironmental implications of charcoals of the Nari Formation in Nari Caldera, Ulleung Island, Korea. *Geosci. J.* **16**, 105–114 (2012).
30. Kim, C. H., Park, J. W., Lee, M. H. & Park, C. H. Detailed bathymetry and submarine terraces in the coastal area of the Dokdo Volcano in the Ulleung Basin, the East Sea (Sea of Japan). *J. Coast Res.* **65**, 523–528 (2013).
31. Choi, B. H., Pelinovsky, E., Kim, D. C., Kim, K. O. & Kim, K. H. Three-dimensional simulation of the 1983 Central East (Japan) Sea earthquake tsunami at the Imwon Port (Korea). *Ocean Eng.* **35**, 1545–1559 (2008).
32. Antranikian, G. et al. Diversity of bacteria and archaea from two shallow marine hydrothermal vents from Vulcano Island. *Extremophiles* **21**, 733–742 (2017).
33. Spietz, R. L. et al. Deep-sea volcanic eruptions create unique chemical and biological linkages between the subsurface lithosphere and the oceanic hydrosphere. *Oceanography* **31**, 128–135 (2018).
34. Dick, G. J. The microbiomes of deep-sea hydrothermal vents: distributed globally, shaped locally. *Nat. Rev. Microbiol.* **17**, 271–283 (2019).

35. German, C. R. et al. Diverse styles of submarine venting on the ultraslow spreading Mid-Cayman Rise. *Proc. Natl Acad. Sci. USA* **107**, 14020–14025 (2010).
36. Inagaki, F. Sulfurimonas autotrophica gen. nov., sp. nov., a novel sulfur-oxidizing -proteobacterium isolated from hydrothermal sediments in the Mid-Okinawa Trough. *Int. J. Syst. Evol. Microbiol.* **53**, 1801–1805 (2003).
37. Takai, K. et al. Sulfurimonas paralvinellae sp. nov., a novel mesophilic, hydrogen- and sulfur-oxidizing chemolithoautotroph within the Epsilonproteobacteria isolated from a deep-sea hydrothermal vent polychaete nest, reclassification of Thiomicrospira denitrificans as Sulfurimonas denitrificans comb. nov. and emended description of the genus Sulfurimonas. *Int. J. Syst. Evol. Microbiol.* **56**, 1725–1733 (2006).
38. Wang, S. et al. Characterization of Sulfurimonas hydrogeniphila sp. nov., a Novel Bacterium Predominant in deep-sea hydrothermal vents and comparative genomic analyses of the genus Sulfurimonas. *Front. Microbiol.* **12**, 626705 (2021).
39. Emerson, D. & Moyer, C. Microbiology of seamounts: common patterns observed in community structure. *Oceanography* **23**, 148–163 (2010).
40. Jiang, C. Y. et al. Alicyclobacillus ferrooxydans sp. nov., a ferrousoxidizing bacterium from solfataric soil. *Int. J. Syst. Evol. Microbiol.* **58**, 2898–2903 (2008).
41. Hemphill-Haley, E. et al. Recent sandy deposits at five Northern California Coastal Wetlands-stratigraphy, diatoms, and implications for storm and tsunami hazards. *Sci. Investig. Rep.-U.S. Geol. Surv.* **2018-5111**, 187 (2019).
42. Kawakami, G. et al. Stratigraphic records of tsunamis along the Japan Sea, southwest Hokkaido, northern Japan. *Island Arc* **26**, e12197 (2017).
43. Goto, T. et al. Tsunami history over the past 2000 years on the Sanriku coast, Japan, determined using gravel deposits to estimate tsunami inundation behavior. *Sediment. Geol.* **382**, 85–102 (2019).
44. Roeber, V. & Bricker, J. D. Destructive tsunami-like wave generated by surf beat over a coral reef during Typhoon Haiyan. *Nat. Commun.* **6**, 7854 (2015).
45. Kim, J.-H., Ho, C.-H., Lee, M.-H., Jeong, J.-H. & Chen, D. Large increase in heavy rainfall associated with tropical cyclone landfalls in Korea after the late 1970s. *Geophys. Res. Lett.* **33**, L18706 (2006).
46. Katsuki, K. et al. Multi-centennial-scale changes in East Asian typhoon frequency during the mid-Holocene. *Palaeogeogr. Palaeoclimatol. Palaeoecol.* **476**, 140–146 (2017).
47. Xue, X. et al. Wave and storm signals in a lacustrine succession and their relationship to paleowind direction (Tanan Depression, Mongolia, early Cretaceous). *Sediment. Geol.* **419**, 105911 (2021).
48. Peters, S. E. & Loss, D. P. Storm and fair-weather wave base: a relevant distinction? *Geology* **40**, 511–514 (2012).
49. Sheik, C. S. et al. Spatially resolved sampling reveals dynamic microbial communities in rising hydrothermal plumes across a back-arc basin. *ISME J.* **9**, 1434–1445 (2015).
50. Molari, M. et al. A hydrogenotrophic Sulfurimonas is globally abundant in deep-sea oxygen-saturated hydrothermal plumes. *Nat. Microbiol.* **8**, 651–665 (2023).
51. Chen, X. Y. et al. Holocene tephrostratigraphy in the East Sea/Japan Sea: implications for eruptive history of ulleungdo volcano and potential for hemispheric synchronization of sedimentary archives. *J. Geophys. Res. Solid Earth* **127**, 1–19 (2022).
52. Kim, G. B., Yoon, S. H., Chough, S. K., Kwon, Y. K. & Ryu, B. J. Seismic reflection study of acoustic basement in the South Korea Plateau, the Ulleung Interplain Gap, and the northern Ulleung Basin: volcano-tectonic implications for Tertiary back-arc evolution in the southern East Sea. *Tectonophysics* **504**, 43–56 (2011).
53. Kim, G. B., Cronin, S. J., Yoon, W. S. & Sohn, Y. K. Post 19 ka B.P. eruptive history of Ulleung Island, Korea, inferred from an intra-caldera pyroclastic sequence. *Bull. Volcano* **76**, 1–26 (2014).
54. Olgun, N. et al. Surface ocean iron fertilization: the role of airborne volcanic ash from subduction zone and hot spot volcanoes and related iron fluxes into the Pacific Ocean. *Glob. Biogeochem. Cycles* **25**, 1–15 (2011).
55. Duggen, S. et al. The role of airborne volcanic ash for the surface ocean biogeochemical iron-cycle: a review. *Biogeosciences* **7**, 827–844 (2010).
56. Censi, P. et al. Trace element behaviour in seawater during Etna's pyroclastic activity in 2001: concurrent effects of nutrients and formation of alteration minerals. *J. Volcanol. Geotherm. Res.* **193**, 106–116 (2010).
57. Jones, M. T. & Gislason, S. R. Rapid releases of metal salts and nutrients following the deposition of volcanic ash into aqueous environments. *Geochim. Cosmochim. Acta* **72**, 3661–3680 (2008).
58. Frogner, P., Gíslason, S. R. & Óskarsson, N. Fertilizing potential of volcanic ash in ocean surface water. *Geology* **29**, 487–490 (2001).
59. Chun, J.-H., Han, S.-J. & Cheong, D.-K. Tephrostratigraphy in the Ulleung Basin, East Sea: Late Pleistocene to Holocene. *Geosci. J.* **1**, 154–166 (1997).
60. Ishihara, T., Sugai, T. & Hachinohe, S. Fluvial response to sea-level changes since the latest Pleistocene in the near-coastal lowland, central Kanto Plain, Japan. *Geomorphology* **147–148**, 49–60 (2012).
61. Koma, T. & Suzuki, Y. Total sulfur content of Late Quaternary sediments in Shibakawa lowland, Saitama Prefecture, central Japan, and its relation to the sedimentary environment. *Chem. Geol.* **68**, 221–228 (1988).
62. Balascio, N. L. et al. A multi-proxy approach to assessing isolation basin stratigraphy from the Lofoten Islands, Norway. *Quat. Res.* **75**, 288–300 (2011).
63. Lim, J. et al. Holocene coastal environmental change and ENSO-driven hydroclimatic variability in East Asia. *Quat. Sci. Rev.* **220**, 75–86 (2019).
64. Nakanishi, R. et al. Holocene tsunami, storm, and relative sea level records obtained from the southern Hidaka coast, Hokkaido, Japan. *Quat. Sci. Rev.* **250**, 106678 (2020).
65. Urabe, A. Reconstruction of tsunami history based on event deposits in the Niigata area, eastern coast of the Sea of Japan. *Quat. Int.* **456**, 53–68 (2017).
66. Wang, S., Jiang, L., Liu, X., Yang, S. & Shao, Z. Sulfurimonas xiamenensis sp. nov. and Sulfurimonas lithotrophica sp. nov., hydrogen- and sulfur-oxidizing chemolithoautotrophs within the Epsilonproteobacteria isolated from coastal sediments, and an emended description of the genus Sulfurimonas. *Int. J. Syst. Evol. Microbiol.* **70**, 2657–2663 (2020).
67. Cai, L., Shao, M.-F. & Zhang, T. Non-contiguous finished genome sequence and description of Sulfurimonas hongkongensis sp. nov., a strictly anaerobic denitrifying, hydrogen- and sulfur-oxidizing chemolithoautotroph isolated from marine sediment. *Stand. Genom. Sci.* **9**, 1302–1310 (2014).
68. Klindworth, A. et al. Evaluation of general 16S ribosomal RNA gene PCR primers for classical and next-generation sequencing-based diversity studies. *Nucleic Acids Res.* **41**, e1 (2013).
69. Lee, I. et al. ContEst16S: an algorithm that identifies contaminated prokaryotic genomes using 16S RNA gene sequences. *Int. J. Syst. Evol. Microbiol.* **67**, 2053–2057 (2017).
70. Parks, D. H., Imelfort, M., Skennerton, C. T., Hugenholtz, P. & Tyson, G. W. CheckM: assessing the quality of microbial genomes recovered from isolates, single cells, and metagenomes. *Genome Res.* **25**, 1043–1055 (2015).
71. Edgar, R. C. Search and clustering orders of magnitude faster than BLAST. *Bioinformatics* **26**, 2460–2461 (2010).

72. McCartney, K. & Wise, S. W. Silicoflagellates and Ebridians from the New Jersey Transect, Deep Sea Drilling Project Leg 93, Sites 604 and 605. in *Initial Reports of the Deep Sea Drilling Project*, *93* (U.S. Government Printing Office, 1987). https://doi.org/10.2973/dsdp.proc.93.127.1987.
73. Hendey, N. I. *An Introductory Account of the Smaller Algae of British Coastal Waters: Part V, Bacillariophyceae [Diatoms*]. (Otto Koeltz Science Publishers, 1964).
74. Round, F. E., Crawford, R. M. & Mann, D. G. *Diatoms: Biology and Morphology of the Genera*. (Cambridge University Press, 1990).
75. Hasle, G. R., Syvertsen, E. E., Steidinger, K. A., Tangen, K. & Tomas, C. R. *Identifying Marine Diatoms and Dinoflagellates*. (Elsevier, 1996).
76. Weltje, G. J. & Tjallingii, R. Calibration of XRF core scanners for quantitative geochemical logging of sediment cores: theory and application. *Earth Planet Sci. Lett.* **274**, 423–438 (2008).

Acknowledgements

This paper has received funding from the Korean Ministry of Science and ICT under the Basic Research Project of the Institute of Geoscience and Mineral Resources (KIGAM) 'Active Tectonics and Development of Fault Segmentation Model for Intraplate Regions' (Grant GP2020-014). It was also supported by a grant from the Nakdonggang National Institute of Biological Resources (NNIBR), funded by the Ministry of Environment (MOE) of the Republic of Korea (NNIBR20242104). We would also like to extend our gratitude to the three anonymous reviewers whose insightful feedback contributed to enhancing the quality of this paper.

Author contributions

Hoil Lee and Yire Choi conceived and designed this study and conducted core sampling through drilling, individual sample sampling, and AMS ^{14}C dating analysis. Furthermore, they investigated three tsunami events inferred and explored the linkage with volcanic activity through the analysis results obtained from the 20HH01 core. Ji Hye Han and Sang Deuk Lee conducted 16 s (v3–v4) Metagenome-seq, Microfossil analysis, and database work. Sujeong Park carried out the data analysis work obtained through XRF core scanning. Hoil Lee wrote the initial draft of the paper. All authors (Hoil Lee, Yire Choi, Ji Hye Han, Sang Deuk Lee, Sujeong Park, and Jin-Hyuck Choi) contributed to interpreting the results and refinement of the paper.

Competing interests

The authors declare no competing interests.

Additional information

Supplementary information The online version contains supplementary material available at https://doi.org/10.1038/s43247-024-01443-2.

Correspondence and requests for materials should be addressed to Yire Choi.

Peer review information *Communications Earth & Environment* thanks Lijiing Jiang, Mitsuru Okono and the other, anonymous, reviewer(s) for their contribution to the peer review of this work. Primary Handling Editors: Carolina Ortiz Guerrero. A peer review file is available.